31st Annual International Conference of the IEEE EMBS
Minneapolis, Minnesota, USA, September 2-6, 2009

Enhancement of the Classification of Multichannel Chromosome Images Using Support Vector Machines

P. S. Karvelis, *Student Member IEEE*, D. I. Fotiadis, *Senior Member, IEEE*, I. Georgiou and P. Sakaloglou.

***Abstract*—Color chromosome classification (karyotyping) allows simultaneous analysis of numerical and structural chromosome abnormalities. The success of the technique largely depends on the accuracy of pixel classification. In this paper we present a method for multichannel chromosome image classification based on support vector machines. First, the image is segmented using a multichannel watershed segmentation method. Classification of the pixels of the segmented regions using support vector machines is then employed. The method has been tested on images from normal cells, showing the improvement in classification accuracy by 10.16% when compared to a Bayesian classifier. The increased classification improves the reliability of the M-FISH imaging technique in identifying subtle and cryptic chromosomal abnormalities for cancer diagnosis and genetic disorders research.**

I. Introduction

THE 46 human chromosomes are the packages that hold the DNA in every cell [1]. They are arranged into 22 pairs of similar, homologous chromosomes and two sex determinative chromosomes (XY: male and XX: female). Numerical or structural abnormalities of chromosomes, which result from an exchange of genetic material between two or more chromosomes, can lead to cancer [2] or other genetic diseases [3]. Usually, the process of determining these abnormalities, by a cytogeneticist, is realized by investigating a number of chromosome images. However, this is a time consuming and laborious procedure that often leads to errors.

Multiplex Fluorescent In Situ hybridization [4,5] (M-FISH) is a multichannel chromosome imaging approach that overcomes many of the previous limitations [6]. More specifically, it uses a number of fluorophores such that each chromosome is stained with a unique combination of the fluorophores. In this way each chromosome is easily identified by its color. For a normal cell, all the pixels in each chromosome should be represented with one identical color. On the other hand, for a cancerous cell, different colors might show up in a chromosome as a result of the chromosomal rearrangements or the exchange of DNA materials between chromosomes. Therefore, by analyzing the color karyotype, geneticists can easily determine if any of the genetic material on the chromosomes has been lost or rearranged, and use it for the study of cancers and genetic disorders. An example of an M-FISH image is shown in Fig. 1 and on the right of the image a chromosome abnormality is shown. From this multiple channel image, it is able to distinguish each human chromosome in a cell by means of a specific color labeling.

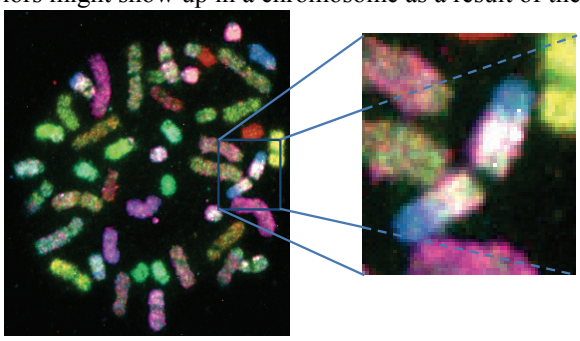

Fig. 1. An M-FISH image and a chromosome abnormality shown by two distinct colors on a chromosome.

Since the birth of the M-FISH technology, many attempts have been proposed that try to automate the process of assigning each chromosome to its class. The methods described in the literature can be classified into two categories:

- Pixel based [7-10]: These methods either classify each pixel of the M-FISH image or create a binary mask of the DAPI image using edge detection algorithms, and classify each pixel of the mask.
- Region based [11-12]: where first the M-FISH image is decomposed into a number of homogenous regions and then are classified to 1 - 24 chromosome classes.

M-FISH imaging promises a rapid and high-resolution genetic diagnosis with the help of automated computer image analysis [13]. The reliability of this molecular diagnosis technique, however, has not reached the level of clinical use [14]. The technique largely depends on the accuracy of pixel classification from the multichannel FISH imaging data. This will become especially challenging when applying the technique to cancerous cells; where it is difficult to determine if the color change in a chromosome is

P.S. Karvelis is with the, Dept. of Computer Science, University of Ioannina, Ioannina, Greece, GR 45110.(e-mail: pkarvel@cs.uoi.gr).

D.I. Fotiadis, is with the Unit of Medical Technology and Intelligent Information Systems, Dept. of Materials Science and Engineering, University of Ioannina, Ioannina, Greece, GR 45110. (corresponding author; tel: 0030-26510-98803; fax: 0030-26510-97092; e-mail: fotiadis@cs.uoi.gr).

I. Georgiou and P. Sakaloglou, is with the Genetics Unit, Dept. of Obstetrics and Gynecology, Medical School, Ioannina, GR 45110 (e-mail: igeorgio@cc.uoi.gr, pr.sakaloglou@gmail.com).

due to the classification error or due to the chromosomal anomalies. Therefore, a crucial step is to improve the pixel-wise classification accuracy.

In this paper we make use of a multichannel watershed based segmentation method in order to segment the image. Then we classify each pixel using Support Vector Machines. Our method consists of a number of steps [12]. First the image is segmented by computing the multichannel gradient magnitude and applying the watershed transform. From each region defined all the pixels are then classified. Our method is compared to a Bayes classifier [7]. This model assumes that each class of chromosomes follows a Gaussian normal distribution in the feature space, which might not be realistic. We introduce a more accurate model based on the support vector machines [20] and a significant improvement in the classification accuracy is reported. A flowchart of the proposed method is shown in Fig. 2.

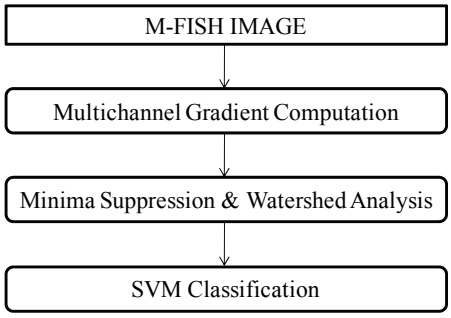

Fig. 2: Flowchart of the proposed methodology.

II. Materials And Methods

A. Multichannel Gradient computation

In order to segment the multichannel chromosome image first we must compute the multichannel gradient magnitude. Instead of separately computing the scalar gradient for each channel DiZenzo [15] introduced a tensor gradient while Drewniok [16] extended this work to multispectral images. Suppose, an M-FISH $I(x,y):\Re^2 \to \Re^5$ since the M-FISH image consists of 5 image channels. Then each pixel of the image is represented by:

$$I(x,y) = \left[I_1(x,y) \quad I_2(x,y) \quad \ldots \quad I_5(x,y) \right]^T, \tag{1}$$

where $I_i(x,y)$, $1 \le i \le 5$ are the components (channels) of the M-FISH image.

Let also the direction v be defined by the angle ω:

$$v = \left[\cos\omega \quad \sin\omega \right]^T, \tag{2}$$

thus the directional derivative of the function $I(x,y)$ is of the form:

$$\frac{\partial I}{\partial v} = \left[\frac{\partial I_1}{\partial v}, \frac{\partial I_2}{\partial v}, \cdots, \frac{\partial I_m}{\partial v} \right]^T = \begin{bmatrix} \nabla I_1 \cdot v \\ \nabla I_2 \cdot v \\ \vdots \\ \nabla I_m \cdot v \end{bmatrix} = \begin{bmatrix} I_1^x & I_1^y \\ I_2^x & I_2^y \\ \vdots & \vdots \\ I_m^x & I_m^y \end{bmatrix} \cdot v = J \cdot v, \tag{3}$$

where $\nabla I_i = \left[I_i^x \quad I_i^y \right] : 1 \le i \le 5$, J is the Jacobian matrix and I_i^x and I_i^y are the derivatives of the i^{th} component in the x and y direction, respectively.

The direction v which corresponds to the maximum of the directional derivative $I(x,y)$ is found, by maximizing the Euclidean norm:

$$\left\| J \cdot v \right\|^2 = (J \cdot v)^T (J \cdot v) = v^T (J^T J) v. \tag{4}$$

The extrema of the quantity $v^T (J^T J) v$, are given by the eigenvalues of the matrix $J^T J$ [16].

B. Minima Suppression and Watershed Analysis

A common problem of the direct application of the watershed transform on the gradient image is the over-segmentation. To overcome this problem a plethora of techniques have been proposed [17]. In our case we have used the grayscale reconstruction [18] of the multichannel gradient magnitude. Grayscale reconstruction reduces a number of unwanted minima, as it provides an intuitive selection scheme controlled by a single parameter.

The next step of our method is the computation of the watershed transform [19]. The watershed transform is a powerful segmentation method which presents some advantages over other developed segmentation methods:

1. The watershed lines form closed and connected regions, where edge based techniques usually define disconnected boundaries which need post-processing to produce closed regions.

2. The watershed lines always correspond to obvious contours of objects which appear in the image.

The output of the WT is a tessellation T_n of the image into its different catchment basins, each one characterized by a unique label:

$$T_n = \{ T_1, T_2, \ldots, T_n \}, \tag{5}$$

where n is the number of the regions.

Only the pixels belonging to the watershed lines are assigned a special label to distinguish them from the catchment basins. The application of the WT to the grayscale reconstructed multichannel gradient magnitude image is illustrated in Fig. 3.

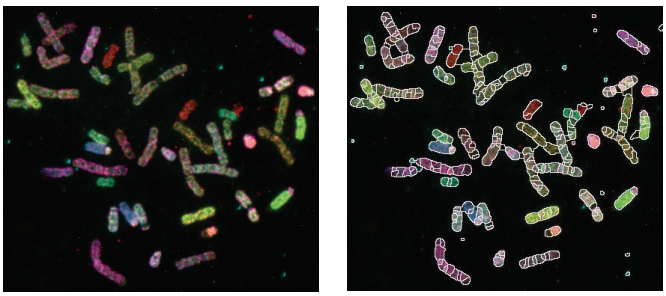

(a) (b)

Fig. 3. M-FISH image segmentation. (a) Initial M-FISH image and (b) Watershed based segmentation.

C. Support Vector Machines

It is considered as a state-of-the-art classifier for both linear and nonlinear classification. SVMs belong to the family of kernel based classifiers. SVMs implicitly map the data into the feature space where a hyperplane (decision boundary) separating the classes may exist. This implicit mapping is achieved with the use of kernels, which are functions that return the scalar product in the feature space by performing calculations in the data space.

The simplest case is a linear SVM [20] trained to classify linearly separable data. Suppose a training data, $\{x_i, y_i\}, \forall i = 1,\ldots,l$, where $x_i \in R^n$, $y_i \in \{-1,1\}$ are the labels for the two classes and l is the number of training data. The training dataset is set to be linearly separable if there exists a vector w and a scalar b such that the below inequalities are valid for all elements of the training set:

$$x_i w + b \geq 1, \quad (6)$$

$$x_i w + b \leq -1. \quad (7)$$

The points, for which the equalities in the above equations are satisfied and have the smallest distance to the decision boundary, are called support vectors. The distance between the two parallel hyperplanes on which the support vectors for the respective classes lie is called the margin. Thus, the SVM finds a decision boundary which maximizes the margin (Fig. 4).

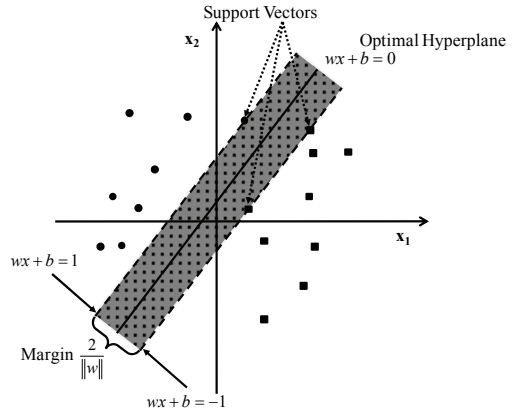

Fig. 4: A hyperplane that maximizes the separating margin between two classes (indicated by data points marked by "■"s and "●"s). Support vectors lie on the boundary hyperplanes of the two classes.

Finding the decision boundary, then it becomes a constrained optimization problem which must minimize $\|w\|^2$ subject to the constraints (Eq. (6) and (7)) and is solved using Lagrange multipliers [21]. The general solution is given:

$$f(x) = \sum_i a_i y_i \langle x_i, x \rangle, \quad (8)$$

where a_i the Lagrange multipliers.

In the case of non-linear classification, kernels are used to map the data into a higher dimensional feature space in which linear classification may be possible. The general solution will be then of the form shown in Eq. (9). Depending on the choice of the kernel function, SVMs can provide both linear and non-linear classification:

$$f(x) = \sum_i a_i y_i K\langle x_i, x \rangle. \quad (9)$$

TABLE I
DIFFERENT TYPES OF KERNELS USED WITH SVMS

Type	Kernel
Linear	$K(x_i, x) = x_i^T x$,
Polynomial	$K(x_i, x) = (\gamma x_i^T x + r)^d, \gamma > 0$,
Radial Basis Function (RBF)	$K(x_i, x) = \exp(-\gamma \|x_i - x\|^2), \gamma > 0$,

where γ, r and d are kernel parameters.

Finally, note that although the SVM classifiers described above are binary classifiers, they are easily combined to handle the multiclass case. A simple, effective combination trains N one-versus-rest classifiers for the N-class case and takes the class for a test point to be that corresponding to the largest positive distance [22]. In this implementation we constructed an RB–SVM by using an RBF as the kernel function.

III. RESULTS

We tested our method on twenty images sets from a public database of 200 hand segmented M-FISH image [23]. The database contains six-channel image sets recorded at different wavelengths. Each dataset includes a "ground truth" image for each M-FISH image in which each pixel is labeled according to the class to which it belongs. This image is labeled such that the gray level of each pixel is its class (chromosome) number. Background pixels are 0 and pixels in a region of overlap are -1. These twenty images are representative [24], and are selected from different probes and focal planes. An extensive study on the clinical feasibility when analyzing cancerous cells will be conducted in the future.

In order to compare our methodology the widely used Bayesian classifier was also implemented [7]. Each pixel is represented by a 5-feature vector z where each feature corresponds to the intensity of one of the 5-image channels. The classifier finds the class for which the *a posteriori* probability is maximized [21, 24]:

$$Decide\ c_i\ if\ P(c_i \mid z) > P(c_j \mid z),\ \forall j \neq i, \quad (10)$$

where $P(c_i \mid z)$ is the *a posteriori* probability, which represents the probability that the feature vector z belongs to chromosome class $c_i, i = 1,\ldots,24$, given the feature vector z.

For training, we have randomly chosen two images [8,12] three times and the rest of the images were used for testing. Thus three different training sets *A*, *B*, and *C* were used.

Thus, there was no overlap between the training and testing data. Each set of the testing images was then classified with respect to each of the training datasets. The classification results obtained from the three trials were then averaged to obtain the final classification results for each test set. The classification results for the various classification schemes are shown in Table II. Fig. 5 presents the classification maps for the two classification schemes.

TABLE II
PERFORMANCE OF SVM VERSUS BAYES CLASSIFICATION

Dataset	Bayes	SVM
A	70.94 ± 6.81	80.20 ± 6.44
B	67.41 ± 7.41	79.57 ± 6.59
C	71.78 ± 7.41	80.83 ± 5.12
Mean	70.04	80.20

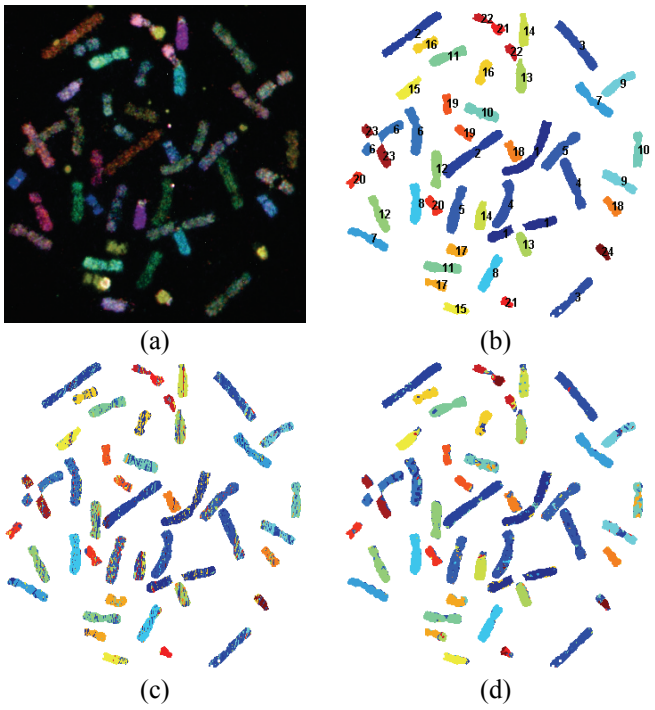

Fig. 5. M-FISH image classification. (a) M-FISH image, (b) Labeled classification map: a separate color was used to represent each chromosome class, (c) Bayes classification map [7], and (d) SVM classification map.

IV. DISCUSSION

We introduced an automatic method for the segmentation and classification of M-FISH chromosome images. The accuracy of the support vector machine classifier is superior to that of the widely used Bayesian [7,8,9,11]. We also introduced a novel segmentation method which \ utilizes both spectral and edge information.

REFERENCES

[1] M. Thompson, R. McInnes and H. Willard, Genetics in Medicine, Ontario, Saunders, 1991.

[2] A. Venkitaraman, "Chromosomal Instability in Cancer: Causality and Interdependence," *Cell Cycle*, vol. 6, pp. 2341 - 2343, 2007.

[3] B. Dave, and W. Sanger, "Role of Cytogenetics and Molecular Cytogenetics in the Diagnosis of Genetic Imbalances," *Sem. in Pediatric Neurology*, vol. 14, pp. 2-6, 2007.

[4] M. R. Speicher, S. G. Ballard, and D. C. Ward, "Karyotyping human chromosomes by combinatorial multi-fluor FISH," *Nature Genetics*, vol. 12, no. 4, pp. 368–375, 1996.

[5] E. Schröck, et al., "Multicolor spectral karyotyping of human chromosomes," *Science*, vol. 273. no. 5274, pp. 494–497, 1996.

[6] T. Veldman, C. Vignon, E. Schröck, J.D. Rowley, and T. Ried, "Hidden chromosome abnormalities in haematological malignancies detected by multicolor spectral karyotyping," *Nat. Genet.*, vol. 15, pp. 406-410, 1997.

[7] M. Sampat, K. Castleman, A. Bovik "Pixel-by-Pixel Classification of MFISH Images," in *Proc. of 24th IEEE EMBS*, Houston, 2002, pp. 999-1000.

[8] M.P. Sampat, A.C. Bovik, J.K. Aggarwal and K.R. Castleman, "Supervised parametric and non-parametric classification of chromosomes images," *Pat. Rec.*, 38(8) pp. 1209-1223, 2005.

[9] W. Schwartzkopf, A.C. Bovik and B.L. Evans, "Maximum-likelihood techniques for joint segmentation-classification of multispectral chromosome images," *IEEE Trans. on Medical Imaging*, 24(12) pp. 1593-1610, 2005.

[10] H. Choi, K. R. Castleman, and A. C. Bovik, "Segmentation and fuzzy-logic classification of M-FISH chromosome images," in *Proc. of IEEE Int. Conf. on Image Proc.*, Atlanta, 2006, pp. 69-72.

[11] K. Saracoglu, J. Brown, L. Kearney, S. Uhrig, J. Azofeifa, C. Fauth, M. Speicher, and R. Eils, "New concepts to improve resolution and sensitivity of molecular cytogenetic diagnostics by multicolor fluorescence in situ hybridization," *Cytometry*, vol. 44, no. 1, pp. 7-15, 2001.

[12] P.S. Karvelis, A. T. Tzallas, D. I. Fotiadis, and I. Georgiou, "A multichannel watershed-based segmentation method for multispectral chromosome classification," *IEEE Trans. on Medical Imaging*, vol. 27, no. 5, pp. 697-708, 2008.

[13] M. R. Speicher, S. G. Ballard and D. C Ward, "Computer image analysis of combinatorial multi-fluor FISH," *Bioimaging*, vol. 4, pp. 52–64, 1996.

[14] C. Lee, et al., "Limitations of chromosome classification by multicolor karyotyping," *American Journal of Human Genetics*, vol. 68, no. 4, pp. 1043–1047, 2001.

[15] S. DiZenzo, "A note on the gradient of a multi-image," *Comput. Vis. Graph. Image Process.*, vol. 33, pp. 116-125, 1986.

[16] C. Drewniok, "Multi-spectral edge detection - Some experiments on data from Landsat-TM," *Intern. J. Remote. Sens.*, vol. 15, no. 18, pp. 3743-3765, 1994.

[17] W. Bieniecki, "Oversegmentation avoidance in watershed-based algorithms for color images," *In Proc. Of Modern Problems of Radio Engineering, Telecommunications and Computer Science*, 2004.

[18] L. Vincent, "Morphological grayscale reconstruction in image analysis: Applications and efficient algorithms," *IEEE Trans. Image Processing*, vol. 2, no. 2, pp. 176-201, 1993.

[19] L. Vincent and P. Soille, "Watershed in digital spaces: An efficient algorithm based on immersion simulations," *IEEE Trans. Pattern Anal. Machine Intel.*, vol. 13, pp. 583-598, 1991.

[20] C. Cortes and V. Vapnik, "Support-vector network", *Mach. Learn.*, vol. 20, pp. 273-297, 1995.

[21] R. Duda, P. Hart, D. Stork, Pattern Classification, *Wiley-Interscience*, 2nd Edition, San Diego, 2000.

[22] S Knerr, L. Personnaz, and G. Dreyfus, "Single layer learning revisited: a stepwise procedure for building and training a neural network," *In Neurocomputing: Algorithms, Architectures and applications*, *Edited by: Fogelman J. Springer-Verlag*; 1990.

[23] http://www.adires.com/05/Project/MFISH_DB/MFISH_DB.shtml

[24] Y. Wang and A. Dandpat, "A hybrid approach of using wavelets and fuzzy clustering for classifying multispectral florescence in situ hybridization images," *Int. Jour. Biom. Imag.*, vol. 2006, 2006.